

Optimising large galaxy surveys for ISW detection

Marian Douspis¹, Patricia G. Castro², Chiara Caprini³, Nabila Aghanim¹

¹ IAS CNRS, Bât. 121, Université Paris-Sud, F-91405 Orsay, France

e-mail: marian.douspis@ias.u-psud.fr, nabila.aghanim@ias.u-psud.fr

² CENTRA, Departamento de Física, Edifício Ciência, Piso 4, Instituto Superior Técnico, Av. Rovisco Pais 1, 1049-001 Lisboa, Portugal. e-mail: pgcastro@ist.utl.pt

³ IPhT, CEA-Saclay, 91191 Gif-sur-Yvette, France
e-mail: chiara.caprini@cea.fr

ABSTRACT

We report on investigations of the power of next generation cosmic microwave background and large scale structure surveys in constraining the nature of dark energy through the cross-correlation of the Integrated Sachs Wolfe effect and the galaxy distribution. First we employ a signal to noise analysis to find the most appropriate properties of a survey in order to detect the correlated signal at a level of more than 4 sigma: such a survey should cover more than 35% of the sky, the galaxy distribution should be probed with a median redshift higher than 0.8, and the number of galaxies detected should be higher than a few per squared arcmin. We consider the forthcoming surveys DUNE, LSST, SNAP, PanSTARRS. We then compute the constraints that the DUNE survey can put on the nature of dark energy (through different parametrizations of its equation of state) with a standard Fisher matrix analysis. We confirm that, with respect to pure CMB constraints, cross-correlation constraints help in breaking degeneracies among the dark energy and the cosmological parameters. Naturally, the constraining capability is not independent of the choice of the dark energy model. Despite being weaker than some other probes (like Gravitational Weak-Lensing), these constraints are complementary to them, being sensitive to the high-redshift behaviour of the dark energy.

Key words. Cosmology – Cosmic microwave background – Large scale structure – Cosmological parameters

1. Introduction

Measurements of the Cosmic Microwave Background (CMB) angular power spectra are now invaluable observables for constraining cosmology. The detailed shape of these spectra allows one to determine cosmological parameters with high precision. The “concordance” model, built over the years with CMB, Supernovae of type Ia, and galaxy distribution observations, seems to reproduce quite well most of the cosmological observables. This model needs the existence of a dark energy component that may be accounted for by a cosmological constant Λ . However, more complex scenarios cannot be ruled out by present datasets. Among them, one could think of a dark energy component with an equation of state w different from $w = -1$ (cosmological constant) or even varying in time $w(z)$ such as in scalar field Quintessence models. Moreover, the effect of dark energy (a recent phase of accelerated expansion) could be mimicked by a deviation from standard gravity at large scales.

To better constrain and understand the present acceleration of the expansion, there is a crucial need for multiple observational probes. The Integrated Sachs-Wolfe (ISW) effect (Sachs & Wolfe 1967) imprinted in the CMB and its correlation with the distribution of matter at lower redshifts (through the galaxy surveys) is one of them. The ISW effect arises from the time-variation of scalar metric perturbations and offers a promising new way of inferring cosmological constraints (e.g. Corasaniti, Gianantonio & Melchiorri 2005, Pogosian et al. 2006). It is usually divided, in the literature, into an early ISW effect and a late ISW effect. The early effect is only important around recombination when anisotropies can start growing and the radiation energy density is still dynamically important. The late ISW effect

originates, on the other hand, long after the onset of matter domination. It is to this latter effect that we refer to here as the ISW effect. The origin of the late ISW effect lies in the time variation of the gravitational potential (e.g. Kofman & Starobinsky 1985, Kamionkowski & Spergel 1994). In a flat universe, the differential redshift of photons climbing in and out of the potential is zero except in a low matter density universe and at the onset of dark energy domination.

The ISW effect is seen mainly in the lowest l -values range of the CMB temperature power spectrum ($l < 30$). Its importance comes from the fact that it is sensitive to the amount, to the equation of state and to the clustering properties of the dark energy. Detection of such a weak signal is, however, limited by cosmic variance. But because the time evolution of the potential that gives rise to the ISW effect may also be probed by observations of large scale structure (LSS), the most effective way to detect the ISW effect is through the cross-correlation of the CMB with tracers of the LSS distribution. This idea, first proposed by Crittenden & Turok (1996), has been widely discussed in the literature (e.g. Kamionkowski 1996, Kinkhabwala & Kamionkowski 1999, Cooray 2002, Afshordi 2004, Hu & Scranton 2004). A detection of the ISW effect was first attempted using the COBE data and radio sources or the X-ray background (Boughn, Crittenden & Turok 1998, Boughn & Crittenden 2002) without much success. The recent WMAP data (Spergel et al. 2003, 2007) provide high quality CMB measurements at large scales. They were used in combination with many LSS tracers to re-assess the ISW detection. The correlations were calculated using various galaxy surveys (2MASS, SDSS, NVSS, APM, HEAO). However, despite numerous attempts in real space (Diego, Hansen & Silk 2003, Boughn &

Crittenden 2004, Cabre et al. 2006, Fosalba & Gaztanaga 2004, Hernandez-Monteagudo & Rubiono-Martin 2004, Nolte et al. 2004, Afshordi, Loh & Strauss 2004, Padmanabhan et al. 2005, Gaztanaga, Maneram & Multamaki 2006, Giannantonio et al. 2006, Rassat et al. 2006) or in the wavelet domain (e.g. Vielva, Martinez-Gonzalez & Tucci 2006, McEwen et al. 2007), the ISW effect is detected through correlations with only weak significance. But the CMB and LSS surveys are now entering a precision age when they can start contributing to a stronger ISW detection, and hence provide valuable cosmological information, in particular about dark energy.

In this work we explore the power of next generation CMB and LSS surveys in constraining the nature of dark energy through the cross-correlation of the ISW effect and the galaxy distribution. We start by using a signal to noise analysis in order to find the most appropriate properties of a survey that will allow to detect the correlated signal at a minimum of 4 sigma. Then we investigate the power of a next generation experiment, obeying the aforementioned characteristics, in constraining different dark energy models.

In Section 2 we revise the auto- and the cross-correlation angular power spectra of the ISW and of the galaxy distributions and model the different contributions entering the analysis. In Section 3 we focus on the signal to noise analysis allowing us to investigate the optimisation of the galaxy survey to the ISW detection. We thus quantify the requirements for an optimal next generation survey planned within the context of the Cosmic Vision call for proposal, namely the DUNE mission (Refregier et al. 2006, <http://www.dune-mission.net/>). In Section 4, we present a Fisher analysis to determine the future constraints on the dark energy equation of state through the correlation between CMB and LSS surveys. Finally we discuss the results and give our conclusions in Section 5.

2. Correlating the ISW effect and galaxy surveys.

The ISW effect is a contribution to the CMB temperature anisotropies that arises in the direction \hat{n} due to variations of the gravitational potential, Φ , along the path of CMB photons from last scattering until now,

$$\frac{\Delta T_{\text{ISW}}}{T}(\hat{n}) = -2 \int_0^{r_0} dr \dot{\Phi}(r, \hat{n}r) \quad (1)$$

where $\dot{\Phi} \equiv \partial\Phi/\partial r$ can be conveniently related to the matter density field δ through the Poisson equation, assuming that the dark energy component does not cluster (for a clustering model see e.g. Weller & Lewis 2003). The variable r is the conformal distance (or equivalently conformal time), defined today as r_0 , and given by

$$r(z) = \int_0^z \frac{dz'}{H_0 E(z')} \quad (2)$$

where, for a Λ CDM cosmology, $E(z)^2 \equiv \Omega_m(1+z)^3 + \Omega_K(1+z)^2 + \Omega_\Lambda$ with Ω_m , Ω_K and Ω_Λ corresponding to the energy density contributions of the matter, the curvature and the cosmological constant today in units of the critical density, and H_0 is the present day Hubble constant. We set $c = 1$. If the dark energy is described by a quintessence field with a present energy density Ω_{DE} and equation of state $w(z)$, then Ω_Λ in $E(z)$ is replaced by $\Omega_{\text{DE}}(1+z)^3 \exp[3 \int_0^z dz' w(z')/(1+z')]$.

In a flat universe ($\Omega_K = 0$), within the linear regime of fluctuations, the gravitational potential does not change in time if

the expansion of the universe is dominated by a fluid of constant equation of state. Therefore, for most of the time since last scattering, matter domination ensured a vanishing ISW contribution. Conversely, however, a detection of an ISW effect would indicate that the effective equation of state of the universe actually changed. This is most interesting in particular with respect to the dark energy dominated era.

It is noteworthy that the temperature change due to the gravitational redshifting of photons in the ISW is frequency independent and cannot be separated from the primary anisotropies using spectral information only.

Since the temperature of the CMB photons is modified, in the dark energy dominated regime, as they traverse an overdensity, the most effective way to detect the ISW effect is through its cross-correlation with the large scale structure distribution. We therefore present in the following the formalism used for computing the cross-correlation signal, as well as the auto-correlations for both galaxies and CMB.

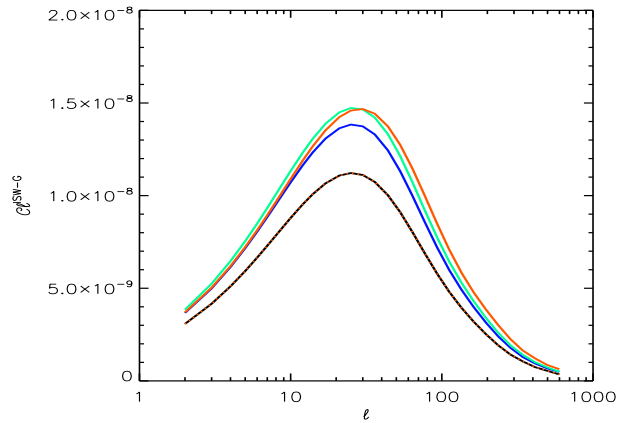


Fig. 1. The angular power spectrum of the correlation between LSS and CMB signals is shown for different cosmologies (see Table 1 for details). The Λ CDM model is shown in black, model A2 in dark blue, model B in green, model C with a transition at $a_t = 0.5$ ($a_t = 0.2$) in red solid (dotted) line.

By expanding the ISW temperature fluctuations in the sky in spherical harmonics, it is straightforward to show that the angular power spectrum of the ISW effect is given by (see e.g. Cooray 2002)

$$C_l^{\text{ISW}} = \frac{2}{\pi} \int dk k^2 P_{\delta\delta}(k) [I_l^{\text{ISW}}(k)]^2, \quad (3)$$

where $P_{\delta\delta}(k)$ is the power spectrum of density fluctuations today, and

$$I_l^{\text{ISW}}(k) = \int_0^{r_0} dr W^{\text{ISW}}(k, r) j_l(kr). \quad (4)$$

The ISW window function, in the case of a spatially flat Universe with non-clustering dark energy, is

$$W^{\text{ISW}}(k, r) = -3\Omega_m \left(\frac{H_0}{k}\right)^2 \dot{F}(r). \quad (5)$$

The j_l are spherical Bessel functions of the first kind and $F(r) \equiv G(r)/a$ is the linear over-density growth factor G divided by the scale factor a . G relates the density field δ at any redshift with its

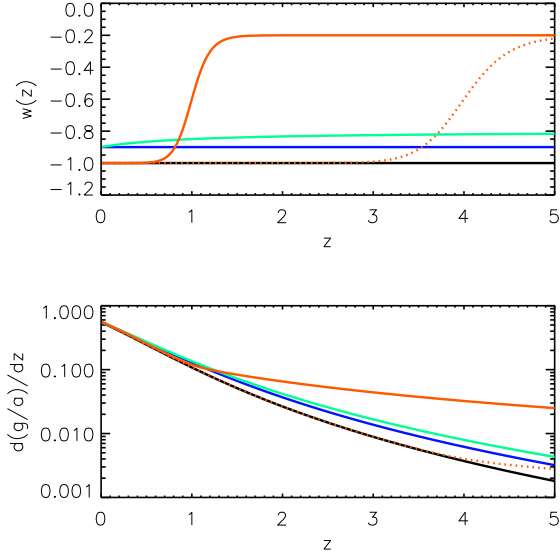


Fig. 2. Top: Dark energy equation of state, following parametrisation A1 (black), A2 (blue), B (green) and C (red) with the cosmological parameters given in Table 1. The dotted line corresponds to a parametrisation C with $a_t = 0.2$; Bottom: corresponding $\dot{F}(z)$ (c.f. Eq. 5)

Model	H_0	Ω_b	Ω_M	σ_8	n_s	w_0	w_a	a_t
A1	73	0.04	0.24	0.74	0.951	-1	—	—
A2	73	0.04	0.24	0.74	0.951	-0.9	—	—
B	73	0.04	0.24	0.74	0.951	-0.9	0.1	—
C	73	0.04	0.24	0.74	0.951	—	—	0.5

Table 1. Values of cosmological parameters for the fiducial models used in the Fisher analysis. Note that we impose flatness for all models.

present day value as $\delta(k, r) = G(r)\delta(k, r=0)$ and, for a Λ CDM cosmology, is given in function of redshift by (see Heath 1977 and Eisenstein 1997)

$$G(z) \propto \Omega_M E(z) \int_z^\infty dz' \frac{1+z'}{E^3(z')}. \quad (6)$$

It is normalized such that $G(z=0) = 1$. In the following, we use Linder approximation for the growth factor (Linder 2005) which writes

$$G(z) \propto \exp \left\{ \int_\infty^z [\Omega_m(z')^\gamma - 1] \frac{dz'}{1+z'} \right\}, \quad (7)$$

where $\Omega_M(z) = \Omega_M \frac{(1+z)^3}{E(z)^2}$ and γ is a parameter set to 0.55 for the Λ CDM model. More generally, $\gamma = 0.55 + 0.05[1 + w(z=1)]$ for an equation of state $w > -1$ and $\gamma = 0.55 + 0.02[1 + w(z=1)]$ for $w < -1$. Equation 7 was shown to be a good approximation to the growth factor for dark energy models with both a constant and a varying equation of state; moreover, it approximates well the growth factor in modified gravity models (e.g. Linder 2005, Amendola, Kunz & Sapone 2007, Huterer & Linder 2007 and references therein).

In the following analysis we consider three parametrisations (A, B, and C) of w , as shown in Fig. 2:

- (A) constant equation of state: $w = -1$ (A1, i.e. the Λ CDM model) and $w = -0.9$ (A2)

- (B) linear evolution with the scale factor: $w(z) = w_0 + w_a \frac{z}{1+z}$
- (C) kink parametrisation, where the equation of state undergoes a rapid transition at a particular redshift z_t : $w(z) = \frac{1}{2}(w_i + w_\infty) - \frac{1}{2}(w_i - w_\infty) \tanh\left(\Gamma \log\left(\frac{1+z_t}{1+z}\right)\right)$. w_i and w_∞ are the two asymptotic values (Douspis et al. 2006, Pogosian et al 2006, Corasaniti et al 2004).

These three parametrizations correspond to three different structure formation histories. The respective growth factor evolution, key ingredient of the ISW effect as shown by Eq. 5, is presented in the bottom panel of Fig. 2.

Going back to Eq. 3, we have defined the power spectrum of density fluctuations by $\langle \delta(\mathbf{k})\delta^*(\mathbf{k}') \rangle = (2\pi)^3 \delta_D(\mathbf{k} + \mathbf{k}') P_{\delta\delta}(k)$ where

$$P_{\delta\delta}(k) \propto 2\pi^2 \left(\frac{k}{H_0} \right)^{n_s+3} \frac{\mathcal{T}^2(k)}{k^3}, \quad (8)$$

with scalar spectral index n_s . The wavenumber k is expressed throughout in $h\text{Mpc}^{-1}$. We use $H_0^{-1} = 2997.9 h^{-1}\text{Mpc}$ as the inverse Hubble distance today. For the transfer function \mathcal{T} we utilise the fitting formulae given in Eisenstein & Hu 1997 for an arbitrary CDM+baryon universe. We use the proportionality symbol in the previous equation because the power spectrum is normalized at small angular scales to the cluster abundances which fix σ_8 , the variance in the mass enclosed in spheres of radius $R = 8h^{-1}\text{Mpc}$. In terms of the power spectrum, we have $\sigma_R^2 = 1/(2\pi)^2 \int k^2 dk P_{\delta\delta}(k) [3H_0 j_1(kR/H_0)/kR]^2$ (see eg Jaffe & Kamionkowski 1998).

Since we are interested in the cross-correlation of the CMB and galaxy distribution in large surveys, we define, in a similar manner, the 2-point angular cross-correlation of the ISW temperature anisotropies with the galaxy distribution field

$$C_l^{\text{ISW-G}} = \frac{2}{\pi} \int dk k^2 P_{\delta\delta}(k) I_l^{\text{ISW}}(k) I_l^{\text{G}}(k), \quad (9)$$

where

$$I_l^{\text{G}}(k) = \int_0^{r_0} dr W^{\text{G}}(k, r) j_l(kr), \quad (10)$$

and the galaxy window function is given by

$$W^{\text{G}}(k, r) = b_{\text{G}}(k, r) n_{\text{G}}(r) G(r). \quad (11)$$

$b_{\text{G}}(k, r)$ is the (in principle) scale- and redshift-dependent bias of the galaxies we consider, and $n_{\text{G}}(z) = n_{\text{G}}(r)/H(z)$ is their normalised redshift distribution defined by

$$n_{\text{G}}(z) = n_{\text{G}}^0 \left(\frac{z}{z_0} \right)^\alpha \exp \left[- \left(\frac{z}{z_0} \right)^\beta \right], \quad (12)$$

where the variables α and β provide a description of the galaxy distribution at low and at high redshifts respectively and z_0 corresponds to the median redshift $z_{\text{med}} \approx 1.4 z_0$. The variable n_{G}^0 is a normalization such that $\int_0^{r_0} n_{\text{G}}(r) dr = 1$.

Examples of the angular power spectrum of the cross-correlation between CMB and galaxy distribution in large surveys are shown in Fig. 1, for the different cosmologies of Table 1. In our analysis we neglect both the presence of massive neutrinos (c.f. Lesgourgues, Valkenburg and Gaztanaga 2007) and magnification effects which are relevant at very high redshift (c.f. LoVerde, Hui and Gaztanaga 2007).

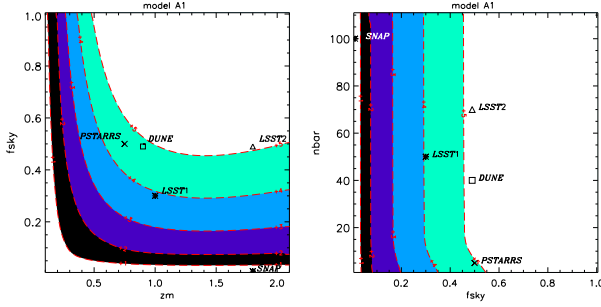


Fig. 3. Total signal-to-noise for a ISW detection in the Λ CDM model (parametrisation A1) as a function of the galaxy survey parameters f_{sky}^c , \bar{N} in units of arcmin^{-2} and z_{med} . The different colours show different levels of detection in number of sigmas.

3. Signal-to-Noise analysis

As a first step, we start by investigating the detection level of the ISW effect in cross-correlation. To do this, we perform a signal-to-noise (SN) analysis. Using the power spectra computed in the previous section we can write the total signal-to-noise of the ISW detection as (Cooray 2002, Afshordi 2004):

$$\left(\frac{S}{N}\right)^2 = f_{\text{sky}}^c \sum_{l=l_{\min}}^{l_{\max}} (2l+1) \frac{[C_l^{\text{ISW-G}}]^2}{[C_l^{\text{ISW-G}}]^2 + (C_l^{\text{ISW}} + N_l^{\text{ISW}})(C_l^{\text{G}} + N_l^{\text{G}})}, \quad (13)$$

where f_{sky}^c is the fraction of sky common to the CMB and the galaxy survey maps, and the total (or cumulative) signal-to-noise is summed over multipoles between $l_{\min} = 2$ and $l_{\max} = 60$ (where the signal has its major contribution). The spectra $C_l^{\text{ISW-G}}$ and C_l^{ISW} were defined in the previous section, and C_l^{G} is straightforward to obtain. The noise contribution in the ISW signal and galaxy surveys are N_l^{ISW} and N_l^{G} respectively. At the scales of interest for the ISW detection, and for the CMB experiment considered, the ISW noise is defined as $N_l^{\text{ISW}} = C_l^{\text{CMB}} + N_l^{\text{CMBexp}}$ where N_l^{CMBexp} is the contribution from the experimental noise. The previous expression is dominated by the sample variance. However, we do include N_l^{CMBexp} in our calculations (as modeled in Knox 1995) for an experiment such as the Planck satellite (see Table 2 for the CMB noise characteristics). The galaxy survey noise is defined by the shot noise contribution: $N_l^{\text{G}} = \frac{1}{\bar{N}}$ where \bar{N} is the surface density of sources per steradian that one can effectively use for the correlation with CMB temperature data. The noise part of the SN depends then, at first order, on the common sky fraction, on the surface density of sources, and on their median redshift through the amplitude of the cross-power spectrum $C_l^{\text{ISW-G}}$ and of the galaxy auto-correlation signal C_l^{G} . With this analysis we are then able to optimise the forthcoming galaxy surveys for an ISW detection in cross-correlation as a function of their three main parameters namely z_{med} , f_{sky}^c and \bar{N} . We use the cosmological parameters values from WMAP3 (Spergel et al 2007) as listed in table 1.

We explore the 3D parameter space, and in Figs. 3, 4 and 5 we show the SN values in 2D diagrams where the third parameter, respectively \bar{N} for the left panel and z_{med} for the right panel, has been marginalised over. In order to have an insight on the detection level of the ISW, we have computed the SN values for

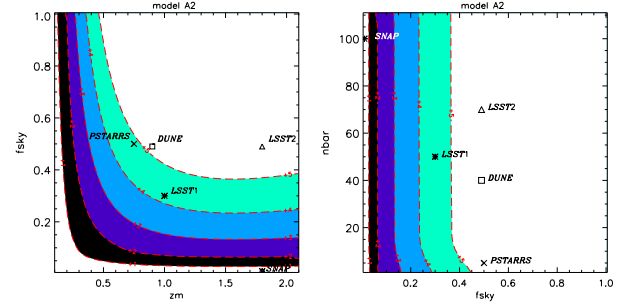


Fig. 4. Total signal-to-noise for a ISW detection in the constant equation of state model with $w = -0.9$ (parametrisation A2) as function of the galaxy survey parameters f_{sky}^c , \bar{N} in units of arcmin^{-2} and z_{med} .

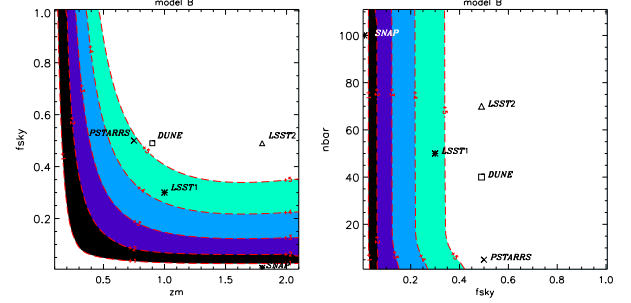


Fig. 5. Total signal-to-noise for a ISW detection in the linearly varying equation of state model (parametrisation B) as function of the galaxy survey parameters f_{sky}^c , \bar{N} in units of arcmin^{-2} and z_{med} .

the dark energy models A and B given in Sect. 2. We do not consider the kink parametrisation (model C) as it gives very similar results to the linear parametrisation. All the results shown in this section were obtained with a redshift and scale independent bias $b_G = 1$ and with the parameters $\alpha = 2$ and $\beta = 1.5$ for the galaxy redshift distribution. This set of parameters is typical for optical galaxies studies (Heavens et al. 2007).

From all these figures, we can see that once the number density of observed sources \bar{N} reaches a given value \bar{N}_{lim} (typically about 10 sources per arcmin^2 or a bit less for all dark energy models), the SN is constant and independent of \bar{N} . This can be understood by going back to the definition of the survey noise (N_l^{G}) entering the SN ratio equation (Eq. 13): in this regime, the contribution from the Poisson noise becomes negligible. As a result, for an equal sky fraction f_{sky}^c and median redshift z_{med} , all surveys satisfying the condition $\bar{N} > \bar{N}_{\text{lim}}$ will give equivalent ISW detections. At a fixed $\bar{N} > \bar{N}_{\text{lim}}$, the SN ratio is on the contrary very sensitive to f_{sky}^c and z_{med} . The former entering the SN through the CMB noise as a multiplicative factor, it is obvious that, for a given z_{med} , the larger f_{sky}^c the higher the detection level. Conversely, at a given f_{sky}^c , increasing z_{med} significantly improves the ISW detection only up to $z_{\text{med}} \sim 1$. In the chosen dark energy model, in fact, dark energy domination always occurs at $z < 1$.

More specifically, in the Λ CDM model a detection of the ISW signal with a confidence of 4σ is attained for median redshifts $z_{\text{med}} > 0.84$ and fractions of sky $f_{\text{sky}}^c > 0.35$. For a constant equation of state model ($w = -0.9$), we find a slightly lower median redshift, of ~ 0.8 , and a slightly lower sky fraction $f_{\text{sky}}^c \sim 0.33$, and the same numbers apply for the varying

equation of state model. The small increase in SN in models A2 and B is expected, since the ISW is an integrated effect. In the last two models, dark energy domination occurs earlier, and structures grow faster. Therefore, they give a stronger contribution to the ISW effect than Λ CDM, providing a better SN for lower median redshift.

In the context of the dark energy models used here, we conclude that in order for a galaxy survey to enable a detection of the ISW effect in cross-correlation with a high enough signal-to-noise ratio it is sufficient to design it based on the predictions from the Λ CDM model. The Λ CDM model gives, in fact, the most conservative detection levels. An optimal survey (with a detection level above 4σ) should thus be designed so that it has a minimum number density of sources of about around 10 galaxy per arcmin⁻², covers a sky fraction of at least 0.35 and is reasonably deep, with a minimum median redshift larger than 0.8. One of the surveys satisfying such conditions and being planned is the DUNE mission proposed to the ESA's Cosmic Vision call for proposal (Refregier et al. 2006, 2008 <http://www.dune-mission.net/>). It will provide a detection of almost 5 sigmas, as shown in the 2D figures together with other future galaxy surveys such as SNAP, PanSTARRS and LSST (see Figs. 3, 4 and 5 and Table 2).

	f_{sky}	z_{med}	nbar (arcmin ⁻²)
DUNE(1)	49%	0.9	40
LSST-1(2)	30%	1	50
LSST-2(3)	49%	1.8	70
SNAP(4)	1 %	1.8	100
PanSTARRS(5)	50%	0.75	5
PLANCK	$f_{\text{sky}} = 80\%$	$\theta_{\text{beam}} = 7\text{arcmin}$	$\omega_r^{-1} = 4e^{-17}$

Table 2. Future LSS surveys characteristics (1) from Refregier et al. 2006, 2008 and the DUNE website, (2) and (3) from Pogorian et al. 2005 as “conservative” and “goal” cases respectively, (4) from the SNAP collaboration, the SNAP website <http://snap.lbl.gov/> and Aldering et al 2007, (5) from Stubbs et al 2007, Heavens et al. 2007 and private communications with S. Phleps. Planck characteristics used for the noise part of the signal-to-noise, and for the Fisher matrices analyses are also given. The values of z_{med} for SNAP and \bar{N} for PanSTARRS are only indicative.

4. Fisher Matrix analysis

In order to quantify the constraint that the cross-correlation of a next generation large scale survey with CMB maps would give on dark energy through the ISW signal we perform a Fisher matrix analysis. For the ISW measurement, such an analytical approach has been shown to yield very accurate error bars by comparison with realistic Monte-Carlo simulations of CMB and galaxy maps by Cabré et al. (2007). We use this technique to compute the errors on a set of cosmological parameters Θ . We assume the usual experimental characteristics, such as the noise and the sky fraction, of Planck and DUNE surveys as listed in Table 2, as these are excellent examples of the next generation of CMB and LSS experiments. They ensure a good SN detection as demonstrated in the previous section.

Given the characteristics of the CMB and the LSS experiments, a fiducial model, and a cosmological framework, the

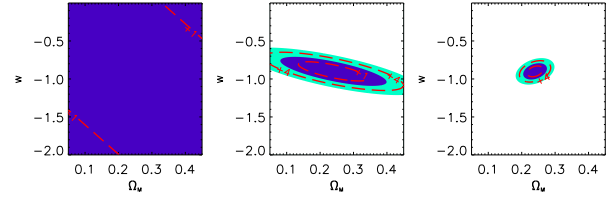


Fig. 6. Two-dimensional marginalised confidence intervals on the plane (Ω_M, w) obtained with a Fisher matrix analysis centered on model A2 with $w = -0.9$. Left: ISW constraints; center: CMB (temperature) constraints; right: combined constraints (see text for details).

smallest possible errors on a set of parameters when determined jointly were shown to be given by the Fisher matrix F elements: $\delta\Theta_i = \sqrt{(F^{-1})_{ii}}$ (see e.g. Tegmark, Taylor and Heavens 1997). In our case, the cross-correlation Fisher matrix for parameters Θ_i and Θ_j is given by

$$F^{i,j} = f_{\text{sky}}^c \sum_l (2l+1) \frac{\partial C_l^{\text{ISW-G}}}{\partial \Theta_i} \text{cov}^{-1}(l) \frac{\partial C_l^{\text{ISW-G}}}{\partial \Theta_j} \quad (14)$$

where

$$\text{cov}(l) = [C_l^{\text{ISW-G}}]^2 + (C_l^{\text{ISW}} + N_l^{\text{CMB}})(C_l^{\text{G}} + N_l^{\text{G}}). \quad (15)$$

The summation is done over the range of multipoles $\sim \pi/(2f_{\text{sky}}^c) < l < 800$. The covariance term, as well as the partial derivatives are evaluated at the fiducial model. See Section 3 (Eq. 13) for more details about the various terms entering the expression.

We assume a flat universe with adiabatic scalar perturbations, a nearly scale invariant initial power spectrum, containing baryonic and cold dark matter, and dark energy. We assume zero curvature since if it were not the case, dark energy would not be distinguishable from the curvature through the ISW effect (Kunz 2007, Clarkson, Cortés & Bassett 2007). The Fisher analysis is then done on the following cosmological parameters: $\Theta = (H_0, \Omega_b, \sigma_8, n_s, \Omega_{\text{DE}})$. In addition, with respect to the dark energy component we study the three scenarios A, B, and C given in Sect. 2 and summarised in Table 1.

We also compute the Fisher matrix corresponding to the constraints imposed by the CMB alone for the same three scenarios. We take into account only one channel, in temperature, following the Planck characteristics listed in Table 2. When combining the constraints from the CMB alone and from the cross-correlation, we consider that the experiments are independent and thus add the corresponding Fisher matrices.

Fig. 6 shows the constraints obtained from the Fisher analyses of model A2 with $w = -0.9$ from the cross-correlation between the CMB and the LSS (left), from the CMB temperature anisotropies alone (middle) and from the combined analysis of both (right). The panels show the confidence intervals that one could obtain on Ω_M and w when other parameters have been marginalised over. As shown in the figure, the constraints from the cross-correlation itself are quite weak, but they play a non obvious and not negligible role in the combination. This is mainly due to the 6-dimensional shape of the likelihood and its degeneracies.

In order to further investigate such a result, we added strong priors on some cosmological parameters to the cross-correlation Fisher matrix (instead of the CMB Fisher matrix). We found that adding a prior on the Hubble constant (H_0), the matter content

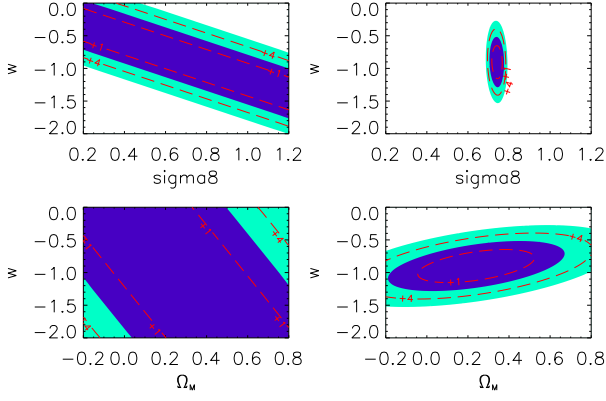


Fig. 7. Two-dimensional marginalised confidence intervals obtained with a Fisher matrix analysis centered on model A2 with $w = -0.9$ for different combinations of parameters: (Ω_M, w) and (σ_8, w) . Left: ISW constraints; right: ISW constraints obtained with a strong prior on σ_8 (see text for details). Note the different scales for Ω_M as compared to Fig. 6.

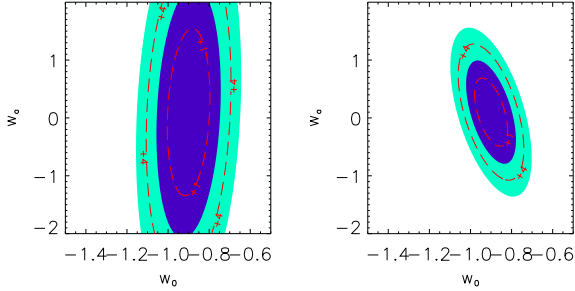


Fig. 8. Two-dimensional marginalized confidence intervals obtained with a Fisher matrix analysis for (w_0, w_a) centered on model B with $w(a) = -0.9 + 0.1(1 - a)$. Left: CMB (temperature) constraints; right: CMB+ISW combined constraints (see text for details).

(Ω_M) , or the spectral index (n_s) does not improve the constraints by much. However, the errors on the dark energy parameters are significantly reduced when adding a prior on the amplitude of the fluctuations via σ_8 . Fig. 7 shows the constraints from the cross-correlation obtained in this last case for scenario A2 ($w = -0.9$) without (left plots) and with (right plots) a strong prior on σ_8 (such that $\sigma_8 = 0.7 \pm 0.02$). The top left panel shows the degeneracy between σ_8 and w and explains why, by constraining strongly σ_8 , with a prior (right panel) or with the CMB (Fig. 6), the equation of state is better determined. This and other minor degeneracy breakings in the 6-dimensional space allows the ISW effect, through cross-correlation, to improve the constraints on dark energy.

As shown previously, the CMB by itself is only able to constrain one parameter of the dark energy model, since it is sensitive mainly to the distance to the last scattering surface (see e.g. Pogosian et al 2006, Douspis et al 2008 and references therein). Therefore, in scenario B with $w(a) = w_0 + (1 - a)w_a$, only the value of the equation of state at present w_0 is constrained (Fig. 8 left). Once again, adding the information coming from the cross-correlation between Planck and DUNE improves slightly the errors on the linear expansion factor w_a (right panel of Fig. 8). However, it does not help to distinguish a constant and a linear dark energy model.

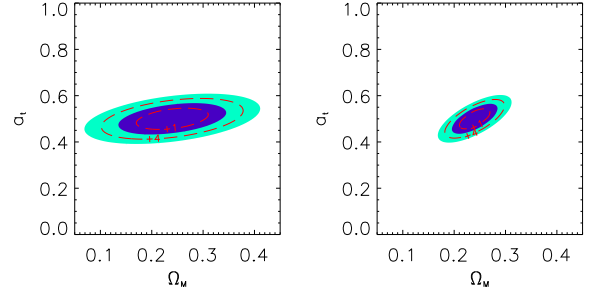


Fig. 9. Two-dimensional marginalized confidence intervals obtained with a Fisher matrix analysis centered for (Ω_M, a_t) on model C with $w(0) = -1$, $w(\infty) = -0.2$ and $a_t = 0.5$; Left: CMB (temperature) constraints; right: combined constraints (see text for details).

Finally we study the “kink” model C in order to assess the sensitivity of the cross-correlation to probe a sharp transition in the evolution of w . The model considered shows a sharp transition ($\Gamma = 10$) between $w(z = 0) = -1$ and some arbitrary value close to 0 far in the past, e.g. $w(z = \infty) = -0.2$. Since with the CMB one can constrain only one dark energy parameter, in this case we choose to let free the transition redshift z_t . For transitions taking place early enough in time, the equation of state is $w = -1$ for most of the period of structure formation. Little difference is then expected between such a model and a Λ CDM model (see Fig. 2). For recent transitions, on the contrary, huge effects are expected. This model has been already investigated in Douspis et al (2008) with current CMB and SNIa data, showing that a transition at $z_t > 0.5$ ($a_t < 0.66$) is allowed. The Fisher matrix analysis, which gives the smallest possible error bar on the parameters, relies by construction on the hypothesis of a Gaussian likelihood for the C_ℓ . This prevents us to have asymmetric error bars on the parameters, and in this particular case does not allow us to obtain the realistic constraints that one could have: i.e., that transitions at $a_t < 0.4$ are also allowed. This can be seen by comparing Fig. 9 (left panel) with Fig. 5 of Douspis et al 2008. Moreover, we choose to take as reference model for scenario C (see Table 1) a reasonable value for the period of transition, $a_t = 0.5$. Due to the big difference of impact on the growth of structure as a function of a_t (see Fig. 2), the errors on the transition period are also strongly dependent on the reference model chosen. In our case, we see in the right panel of Fig. 9 that adding the ISW information to the CMB temperature anisotropy improves the constraints on Ω_M in the plane (Ω_M, a_t) , but does not improve constraints on a_t .

5. Conclusions

In this work we have analysed the cross-correlation between the ISW effect and a galaxy survey characterised by the redshift distribution given by the Eq. 12 and assuming simple Poisson noise. We have relied on Linder approximation given in Eq. 7 to model the growth of structure in dynamical dark energy models.

We have determined the most appropriate properties of a survey in order to detect an ISW signal in cross-correlation CMB/LSS at a minimum of 4 sigma. To do this we have used a signal to noise analysis. Our results agree with those obtained by Afshordi (2004): we have shown that the necessary properties for a survey to be significantly successful in the quest for an ISW signal are a minimum number density of sources of about 10 galaxies per arcmin², a minimum sky fraction of the order of

0.35 and a minimum median redshift of about 0.8. We indicate the DUNE project as a promising candidate for providing a good ISW detection, once correlated with Planck data. Furthermore, the number of galaxies detected by such a survey is high enough to divide the distribution in different redshift bins, allowing to probe the dark energy at different epochs. As found above, the Poisson noise is negligible for a number of detected galaxies which is higher than 10 per arcmin⁻². If this condition is met in each redshift bin, this increases the signal to noise correspondingly to the number of bins considered.

We then investigated the power in constraining different dark energy models of typical next generation experiments having the aforementioned characteristics. We took the DUNE and the Planck surveys. Here again, we confirm the result of previous analyses, such as those of Pogosian et al (2006) and Douspis et al (2008). We showed that the ISW effect does help (as compared to CMB alone) in breaking degeneracies among the parameters describing the dark energy model and the other cosmological parameters, primarily σ_8 . The cross-correlation allows us to put a constraint of the order of 10% on w for a model with a constant equation of state (A) and reduces the errors on the estimation of the parameter w_a in a linear model (B). However, it does not permit to distinguish between a constant and a dynamical equation of state for the dark energy. Fitting a dark energy model with a kink, we have found that adding the cross-correlation does not improve the CMB constraints on the transition redshift: the ISW is therefore insensitive to sharp transitions, and a transition at any redshift larger than 0.5 is still allowed.

Acknowledgements. NA and MD thank the collaboration programme PAI-PESOA for partial funding. They further thank Instituto Superior Técnico (IST) for hospitality. PGC is funded by the *Fundação para a Ciência e a Tecnologia* and wishes to thank the Institut d'Astrophysique Spatiale (IAS) for its welcoming and support, and Stefanie Phleps for useful conversations. CC acknowledge support by the ANR funding PHYS@COL&COS, and thanks IAS and IST for hospitality. We thank Mathieu Langer for helpful comments.

References

- Afshordi, N., Loh, Y. & Strauss, M.A., Phys. Rev. D, 69, 083524 (2004)
 Afshordi, N., Phys. Rev. D, 70, 083536 (2004)
 Aldering, G. et al., Astropart. Phys., 27, 213 (2007)
 Amendola, L., Kunz, M. & Sapone, D., arXiv:0704.2421
 Boughn, S.P., Crittenden, R.G. & Turok, N.G., New Astron., 3, 275 (1998)
 Boughn, S.P. & Crittenden, R.G., Phys. Rev. Lett., 88, 021302 (2002)
 Boughn, S.P. & Crittenden, R.G., Nature, 427, 45 (2004)
 Cabré, A. et al., arXiv:astro-ph/0701393
 Cabré, A. et al., Mon. Not. Roy. Astron. Soc. Lett., 372, L23 (2006)
 Clarkson, A., Cortés, M. & Bassett, B., J. Cosm. Astropart. Phys., 0708:011 (2007)
 Corasaniti, P. et al., Phys. Rev. D, 70, 083006 (2004)
 Corasaniti, P., Gianantonio, T. & Melchiorri, M., Phys. Rev. D, 71, 123521 (2005)
 Cooray, A., Phys. Rev. D, 65, 103510 (2002)
 Crittenden, R.G. & Turok, N.G., Phys. Rev. Lett., 76, 575 (1996)
 Diego, J., Hansen, H. & Silk, S., Mon. Not. Roy. Astron. Soc., 338, 796 (2003)
 Douspis, M. et al, accepted in A&A, 2008, arXiv:astro-ph/0602491
 Eisenstein, D.J., arXiv:astro-ph/9709054
 Eisenstein, D.J. & Hu, W., Astrophys. J., 496, 605 (1998)
 Fosalba, P. & Gaztanaga, E., Mon. Not. Roy. Astron. Soc., 350, L37 (2004)
 Gaztanaga, E., Maneram, M. & Multamaki, T., Mon. Not. Roy. Astron. Soc., 365, 171 (2006)
 Giannantonio, T. et al., Phys. Rev. D, 74, 063520 (2006)
 Heath, D.J., Mon. Not. Roy. Astron. Soc., 179, 351 (1977)
 Heavens, A.F., Kitching, T.D., Verde, L., arXiv:astro-ph/0703191
 Hernandez-Monteagudo, C. & Rubino-Martin, J.A., Mon. Not. Roy. Astron. Soc., 347, 403 (2004)
 Hu, W. & Scranton, R., Phys. Rev. D, 70, 123002 (2004)
 Huterer, D. & Linder, E.V., Phys. Rev. D, 75, 023519 (2007)
 Kamionkowski, M. & Spergel, D.N., Astrophys. J., 432, 7 (1994)
 Kamionkowski, M., Phys. Rev. D, 54, 4169 (1996)
 Kinkhabwala, A. & Kamionkowski, M., Phys. Rev. Lett., 82, 4172 (1999)
 Knox, L., Phys. Rev. D, 52, 4307 (1995)
 Kofman, L.A. & Starobinsky, A.A., Soviet. Astron. Lett. (Tr:Pisma), 11, 5, 271 (1985)
 Kunz, M., arXiv:astro-ph/0702615
 Jaffe, A.H. & Kamionkowski, M., Phys. Rev. D, 58, 043001 (1998)
 Lesgourgues, J., Valkenburg, W. & Gaztanaga, E., arXiv:0710.5525
 LoVerde, M., Hui, L. & Gaztanaga, E., Phys. Rev. D, 75, 043519 (2007)
 Linder, E.V., Phys. Rev. D, 72, 043529 (2005)
 McEwen J. D. et al., Mon. Not. Roy. Astron. Soc., 373, 1211 (2007)
 Nolta, M.R. et al., Astrophys. J., 608, 10 (2004)
 Padmanabhan, N. et al., Phys. Rev. D, 72, 043525 (2005)
 Pogosian, L. et al., Phys. Rev. D, 72, 103519 (2005)
 Rassat, A. et al., Mon. Not. Roy. Astron. Soc., 377, 1085 (2007)
 Refregier, A. et al., arXiv:astro-ph/0610062
 Refregier, A. et al., submitted to Experimental Astronomy, 2008
 Sachs, R.K. & Wolfe, A.M., Astrophys. J., 147, 73 (1967)
 SNAP Collaboration (J. Albert et al.), SLAC-PUB-11393 (2005)
 Spergel, D.N. et al., Astrophys. J. Supp., 148, 175 (2003)
 Spergel D.N. et al., Astrophys. J. Supp., 170, 377 (2007)
 Stubbs, C.W. et al., Publ. Astron. Soc. Pac., C119, 1163 (2007)
 Tegmark, M., Taylor, A. & Heavens, A., Astrophys. J., 480, 22 (1997)
 Tyson, J.A. for the LSST Collaboration, arXiv:astro-ph/0609516
 Vielva, P., Martinez-Gonzalez, E. & Tucci, M., Mon. Not. Roy. Astron. Soc., 365, 891 (2006)
 Weller, J. & Lewis, A., Mon. Not. Roy. Astron. Soc., 346, 987 (2003)